

Performance and Reliability Monitoring of Ship Hybrid Power Plants

© Charalampos Tsoumpris, © Gerasimos Theotokatos

University of Strathclyde Glasgow, Maritime Safety Research Centre, Department of Naval Architecture, Ocean and Marine Engineering, United Kingdom

Abstract

Recently, the marine industry has been under a paradigm shift toward adopting increased automation, and initiatives to enable the autonomous operations of ships are ongoing. In these cases, power plants require advanced monitoring techniques not only for the performance parameters but also to assess the health state of their critical components. In this respect, this study aims to develop a monitoring functionality for power plants that captures the performance metrics while considering the overall system and its components' reliability. A hybrid power plant of a pilot boat is considered a case study. A rule-based energy management strategy is adopted, which makes the decisions on the power distribution to the investigated power plant components. Additionally, a dynamic Bayesian network is developed to capture the temporal behavior of the system's/components' reliability accounting for the power plant's operating profile. Results demonstrate that the selected hybrid power plant monitoring capabilities are enhanced by providing the power plant performance along with the estimation of the system's health state. Furthermore, these extended monitoring capabilities can provide the essential metrics to facilitate decisionmaking, enabling the autonomous operation of the power plant.

Keywords: Hybrid power plant, Monitoring, Energy management, Dynamic Bayesian network, Autonomous operations

1. Introduction

As technological breakthroughs have been maturing, modern vessels incorporate smart technologies capable of performing various automated tasks [1]. Adopting smart sensors and systems onboard ships enables increased monitoring capabilities, which is crucial for next-generation autonomous ships to perform autonomous decision-making actions. Several research projects have been investigating and developing technologies to enable autonomous shipping. Specifically, AUTOSHIP has been focused on developing and applying key enabling technologies in two autonomous ships, highlighting the importance of autonomous machinery systems with predictive condition monitoring capabilities [2]. Furthermore, MUNIN provided a concept for an autonomous ship, pinpointing the importance of an intelligent machinery system that can perform monitoring tasks with advanced failure predetection and handling functionalities [3].

The power plant operation of modern ships is already highly automated. Sensors are installed to monitor the performance of the majority of the power plant components. Usually, the acquired data are pertinent to performance measurements, including fuel consumption and emissions [4]. Nevertheless, smart ships require extended monitoring capabilities to assess the health state of their power plants.

In this respect, traditional metrics or key performance indicators are insufficient to capture the plant's health state. Data from sensors can enable diagnostic functionalities in the power plant while also being employed to estimate the health state and determine the remaining useful life (RUL) of the investigated components or system [5]. Automotive and aerospace industries already employ several methods to estimate the health state and perform future predictions using the prognostics and health management framework [6]. However, the maritime industry lags in terms of using similar methods. Gkerekos et al. [7] proposed an approach



Address for Correspondence: Charalampos Tsoumpris, University of Strathclyde Glasgow, Maritime Safety Research Centre, Department of Naval Architecture, Ocean and Marine Engineering, United Kingdom
E-mail: charalampos.tsoumpris@strath.ac.uk
ORCID ID: orcid.org/0000-0002-2808-9858

Received: 30.11.2021
Accepted: 04.01.2022

To cite this article: C. Tsoumpris, and G. Theotokatos, "Performance and Reliability Monitoring of Ship Hybrid Power Plants." *Journal of ETA Maritime Science*, vol. 10(1), pp. 29-38, 2022.

©Copyright 2022 by the Journal of ETA Maritime Science published by UCTEA Chamber of Marine Engineers

to monitor the machinery's health state using vibration data. Lazakis et al. [8] used a dynamic time series neural network to predict future operating values of ship machinery critical systems. Using a similar approach, Zaman et al. [9] applied a condition monitoring approach using neural networks on the main engine to predict future variations of performance parameters while combining reliability tools for criticality assessment. In Kökkülünk et al. [10], a mathematical model to estimate engine degradation was developed under varying operating conditions. Nevertheless, the aforementioned studies typically focused on calculating the health state of a particular component or individual system without incorporating insight into the power plant as an integrated system.

Moreover, for the successful operation of unmanned missions, Edge et al. [11] argued that priority should be given to the selection and optimization of the machinery design in respect to the availability. Pertinent literature reports attempted to monitor autonomous power plants operations. Abaei et al. [12] developed a probability model based on the multinomial process tree and hierarchical Bayesian model to evaluate the reliability of an unattended machinery plant under the influence of random events. Ellefsen et al. [13] acknowledged the potential of using deep learning techniques to estimate the RUL of autonomous systems in real time from measured shipboard data. Bolbot et al. [14] introduced the concept of a safety monitoring system in cruise ship power plants to estimate the probability of blackout using sensor measurements. Utne et al. [15] highlighted the importance of dynamic risk monitoring and control in autonomous marine systems, although these tools have not been currently implemented in the maritime sector.

From the preceding studies, the following research gaps are identified: (a) a systematic and structured framework to monitor the machinery health state in the maritime industry is not available, (b) the influence of the performance profile on the health state of the components have not been

investigated, and (c) the overall system's dynamic health state estimation based on an actual operational profile has not been addressed.

In this respect, this study aims to develop a monitoring functionality for power plants that captures performance metrics while considering the overall system and its components' reliability as health indicators. Modeling of the power plant's performance is done using a combination of the first principles method, look-up tables, and built-in Simulink blocks. The reliability of the power plant's components is calculated using failure rates based on the proportional hazard model (PHM), while the system's reliability is calculated using a dynamic Bayesian network (DBN). A parallel hybrid power plant of a pilot boat is selected as a case study.

2. Methodology Overview

The methodological steps to develop the monitoring functionality are presented herein. The first step is to develop a rule-based energy management strategy that defines the operating setpoints for the power plant components. Subsequently, performance models are employed to estimate the power plant's behavior. In the next step, the power plant's operating points are fed into the PHM to update the failure rate and calculate the components' reliability. Finally, using the components' reliability, the system reliability is calculated using the DBN.

3. System Description & Performance Modeling

In this study, a parallel hybrid power plant of a pilot boat is selected to demonstrate the proposed methodology's applicability. Figure 1 shows a schematic representation of the power plant's configuration. The hybrid power plant is a combination of a diesel engine, a battery, and an electric machine. The diesel engine and the electric machine are coupled via a gearbox. The electric machine can be used as a power take in (PTI) to supply propulsive power and as a power take off (PTO) to charge the battery. Table 1 presents the power plant's components' characteristics.

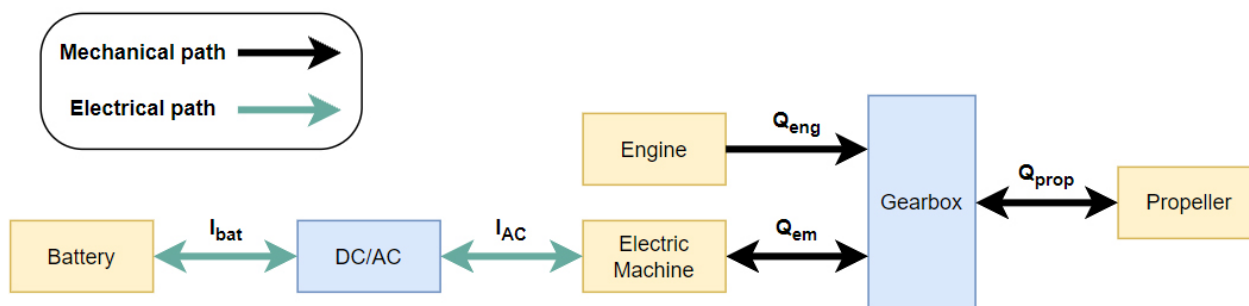


Figure 1. Parallel hybrid power plant configuration

Table 1. Component's characteristics

Component	Parameter	Value
Engine	Type	4 stroke, 8 cylinders
	Power MCR (kW)	423
	Speed MCR (RPM)	2100
Electric machine	Nominal power (kW)	100
Battery	Type	Lithium ion
	Module capacity (Ah)	100
	Nominal voltage (V)	12
	Number of modules	100
MCR: Maximum continuous rating		

The investigated hybrid power plant is modeled in MATLAB/Simulink environment using a modular approach. Each power plant component is modeled as a separate block, and connections facilitate the parameters' exchange between the interconnected components.

3.1. Diesel Engine Modeling

The performance of the diesel engine is modeled by employing the mean value engine model proposed by Theotokatos [16]. The engine brake mean effective pressure is calculated by subtracting the friction mean effective pressure (FMPE) from the indicated mean effective pressure (IMEP). The FMPE is considered a function of the IMEP and the engine crankshaft rotation speed, whereas the IMEP is calculated using the rack position, the maximum IMEP, and the combustion efficiency.

The torque produced by the engine is calculated using the following equation:

$$Q_{eng} = \frac{BMEP V_D}{2\pi rev_{cy}} \quad (1)$$

where rev_{cy} is the number of crankshaft revolutions per cycle.

The engine fuel mass flow rate is calculated as:

$$\dot{m}_f = \frac{z_{cyl} m_{f,cyl} N_{eng}}{60 rev_{cy}} \quad (2)$$

where z_{cyl} denotes the cylinder number and $m_{f,cyl}$ is the mass of injected fuel per cylinder per cycle, the variation of which versus the engine rack position is provided as input.

The following equations are employed to calculate the engine brake power and brake specific fuel consumption (BSFC):

$$P_b = \frac{\pi N_{eng} Q_{eng}}{30} \quad (3)$$

$$BSFC = \frac{\dot{m}_f}{P_b} \quad (4)$$

The engine governor is modeled using a proportional-integral (PI) controller law [16].

3.2. Electric Machine Modeling

For the modeling of the electric machine, a quasi-static approach is followed, which is widely used in supervisory automotive control applications [17,18]. Energy losses are calculated based on the operating point of the electric machine [19]. The power output is then expressed as:

$$P_{em} = \frac{1}{\eta_{em} (N_{em}, P_{elec})} \frac{\pi N_{em} Q_{em}}{30}, P_{elec} \geq 0 \text{ (Motor Mode)} \quad (5)$$

$$P_{em} = \eta_{em} (N_{em}, P_{elec}) \frac{\pi N_{em} Q_{em}}{30}, P_{elec} < 0 \text{ (Generator Mode)} \quad (6)$$

where η_{em} is the efficiency of the electric machine, which is considered a function of its speed and electric power.

The desired power output of the electric machine is controlled using a similar (PI) controller approach as in the case of the diesel engine.

3.3. Battery

The power plant battery is considered to be of the lithium ion type with 100 modules. To model the battery's behavior while charging and discharging, the built-in Simscape model proposed by Tremblay and Dessaint [20] was employed. Specifically, the battery's voltage in discharge and charge is respectively obtained by the following equations:

$$V_{bat} = E_0 - R i - K \frac{Q}{Q - i t} (i t + i^*) + A \exp(-B i t),$$

$$i^* > 0 \text{ (Discharge)} \quad (7)$$

$$V_{bat} = E_0 - R i - K \frac{Q}{i t - 0.1 Q} i^* - K \frac{Q}{Q - i t} i t + A \exp(-B i t),$$

$$i^* < 0 \text{ (Charge)} \quad (8)$$

where V_{bat} is the battery voltage, E_0 is the battery constant voltage, K is a polarization constant, Q is the battery capacity corresponding to the actual battery charge, A is the exponential zone amplitude, B is the exponential zone time constant inverse, R is the internal resistance, i is the actual battery charge ($\int i dt$), i is battery current, and i^* denotes the filtered current.

3.4. Gearbox

The following equation derived from angular momentum conservation in the gearbox is used to calculate the engine speed:

$$\frac{dN_{eng}}{dt} = \frac{30(\eta_{gb} (Q_{eng} - Q_{em}) - Q_{prop})}{\pi(I_{eng} + I_{em} + I_{gb} + I_{prop})} \quad (9)$$

where η_{gb} denotes the gearbox efficiency and I_{eng} , I_{gb} , I_{em} and I_{prop} are the polar moments of the inertia of the engine, electric machine, gearbox, and propeller, respectively.

3.5. Propeller

Finally, the propeller law is utilized to calculate the propeller torque. To calculate the constant parameter k_p , the engine torque and speed at the maximum continuous rating (MCR) are used. As a result, the propeller torque is expressed as:

$$Q_{prop} = k_p N_{eng}^2 \quad (10)$$

4. Rule-based Energy Management

Since the power plant consists of a parallel hybrid configuration, a supervisory control strategy must be adopted to allocate the load to various power sources [21]. This study adopts a rule-based energy management strategy (RB-EMS) to specify the operating mode (e.g., hybrid and electric) and the components' operating point. This strategy is implemented using the Stateflow state machine in Simulink, which can be used to develop a decision logic and supervisory control strategies for hybrid systems [22].

The power plant can switch between different modes including hybrid, fully electric, and mechanical. Similar approaches have been presented in the pertinent literature [23,24]. Table 2 presents the decision logic. It must be noted that the mechanical mode is included in the hybrid mode with the electric machine switched off.

Table 2. Rule-based energy management strategy

Requested engine speed (rev/min)	State of charge		
	0-40	40-80	80-100
0-1000	Hybrid	Electric	Electric
1000-1400	Hybrid	Hybrid	Electric
1400-2100	Hybrid	Hybrid	Electric
The mechanical mode is included in the hybrid mode with the electric machine switched off			

After the operating mode is defined, the operating point of every component is specified. When the engine is switched on, it is set to operate at the optimal (BSFC) point in the current engine speed. In case of surplus power, it is used to charge the battery and the electric machine operates in the PTO mode. In contrast, when the engine load is not sufficient to satisfy the propeller demand, the electric machine is used in the PTI mode.

5. Reliability Modeling

5.1. Dynamic Bayesian Networks

To capture the health state of the investigated system and its components, reliability is used as a metric to demonstrate

degradation. Mathematically, reliability is defined as the probability that a component is functioning at the time interval $(0,t)$, where t is the mission time [25]. As a result, reliability can be used as an alternative to describing the degradation function [26].

In this study, a DBN approach is used. DBNs are an extension of the conventional Bayesian network (BN) that can capture the temporal behavior of the network, as they can predict future node probabilities based on the feeding evidence [27].

A BN is a pair of a directed acyclic graph (DAG) and a joint probability distribution function that satisfies the Markov condition [28]. The DAG is defined by nodes (V) and edges (E) where nodes are random variables and edges show the probabilistic relationships between the nodes.

The BN consists of the qualitative part, where the topology of the network is represented by the DAG, and the quantitative part, where conditional probabilities are specified to make the numerical inference [29]. The joint probability distribution function of the network is calculated as the product of all conditional probability density functions of each node given all its parent nodes as follows [30]:

$$P(X_1, X_2, \dots, X_n) = \prod_{i=1}^n P(X_i | Pa(X_i)) \quad (11)$$

where $Pa(X_i)$ represents the parent set of variable X_i and $P(X_i | Pa(X_i))$ is the conditional probability distribution function of variable X_i given its parent set.

The limitation of the conventional BN is its inability to capture temporal relationships between the nodes of the network, resulting in a static representation of the joint probability distribution function at a specific time instant [28]. To overcome this limitation, DBN were introduced, which can provide temporal dependencies of network nodes considering the previous time slice. The joint probability distribution function of the DBN network from the previous time slice to the current time slice can be expressed as [27]:

$$P(Z_t | Z_{t-1}) = \prod_{i=1}^n P(Z_{i,t} | Pa(Z_{i,t})) \quad (12)$$

where Z is the family of random variables X_1, X_2, \dots, X_N , $Z_{i,t}$ is the i th node at the time slice t , and $Pa(Z_{i,t})$ is the parent nodes of $Z_{i,t}$ from the same and previous time slices.

Finally, the following equation is employed to calculate the overall joint probability distribution function of the DBN from the first time slice till slice N :

$$P(Z_{1:N}) = \prod_{t=1}^N \prod_{i=1}^n P(Z_{i,t} | Pa(Z_{i,t})) \quad (13)$$

5.2. Failure Rate Update Model

The failure (or hazard) rate is used to calculate the reliability of the power plant's components. This study considers the operating point (load) of the components as a factor that influences the failure rate. Usually, in health-aware control applications, PHMs are used, which take into account the actuators' control effort in the degradation function [26,31]. The PHM was first introduced by Cox [32] and employs the following expression for the calculation of the failure rate:

$$\lambda(t, l) = \lambda_0(t)g(l, \vartheta) \quad (14)$$

where λ_0 is the nominal failure rate dependent on time only and $g(l, \vartheta)$ is the covariate function that depends on covariate l that affects the component and an unknown parameter θ of the component model. The term $g(l, \theta)$ can take many forms [33]. However, the linear form is considered herein.

In this study, the Weibull PHM (WPHM) proposed by Gorjian et al. [34] is used, which is an extension of the PHM. The failure rate is assumed to follow the Weibull distribution, resulting in an increasing failure rate with time when the shape factor β is greater than one. According to the WPHM, the failure rate is calculated as follows:

$$\lambda(t, l) = \beta \lambda_0^\beta t^{\beta-1} g(l, \vartheta) \quad (15)$$

Failure rates that are used in this study are based on the OREDA 2015 database [35]. In particular, the components' mean and maximum failure rates are considered. Because the Weibull distribution is followed, a correction procedure for the failure rates is followed according to [36], since the failure rates in the OREDA are assumed constant.

For the diesel engine, it is assumed that the failure rate is the mean of the values provided in the OREDA in the region close to the half load region, whereas it reaches its maximum

value in the idle and at full load regions. Consequently, the engine failure rate is calculated by the following equations:

$$\lambda(t, l) = \beta \lambda_{mean}^\beta t^{\beta-1} \left(\left(\frac{\lambda_{max}}{\lambda_{mean}} \right)^\beta + \left(1 - \left(\frac{\lambda_{max}}{\lambda_{mean}} \right)^\beta \right) \frac{l}{0.4} \right), \quad 0 \leq l < 0.4 \quad (16)$$

$$\lambda(t, l) = \beta \lambda_{mean}^\beta t^{\beta-1}, \quad 0.4 \leq l < 0.6 \quad (17)$$

$$\lambda(t, l) = \beta \lambda_{mean}^\beta t^{\beta-1} \left(1 + \left(\left(\frac{\lambda_{max}}{\lambda_{mean}} \right)^\beta - 1 \right) \frac{l-0.6}{0.4} \right), \quad 0.6 \leq l < 1 \quad (18)$$

For other components, it is assumed that the failure rate is calculated according to Equation (19). The mean failure rate value was considered as reported in the OREDA, whereas it increases as a function of the load till the full load, where it gets its maximum value.

$$\lambda(t, l) = \beta \lambda_{mean}^\beta t^{\beta-1} \left(1 + \left(\left(\frac{\lambda_{max}}{\lambda_{mean}} \right)^\beta - 1 \right) l \right) \quad (19)$$

6. Case Study

6.1. Operating Profile

To demonstrate the applicability of the proposed approach, an operating profile that specifies the time variation of the propeller power and speed setpoints is required. Operating data from an actual pilot boat representing the time variation of the engine speed is shown in Figure 2.

Due to the inherent noise of the collected data, this profile was elaborated and was converted into power setpoints for the rule-based energy management strategy. Additionally, the profile corresponding to a one-month operation was developed based on these setpoints and considering a random variation of $\pm 10\%$. This randomness was included

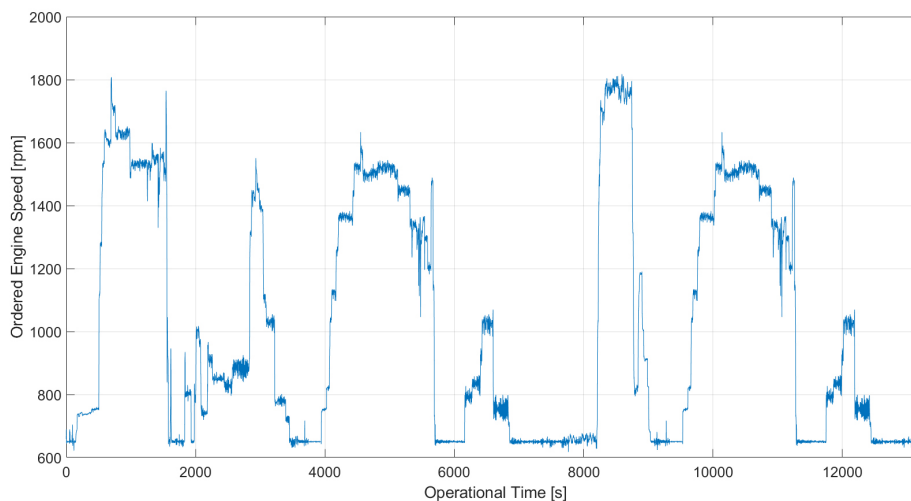


Figure 2. Actual operating profile of the pilot boat engine case study

to derive a more realistic scenario. Figure 3 provides the developed operating profile for 6 hours as the one-month operating profile cannot be readily presented in a single plot.

Finally, an overall model screenshot is presented in Figure 4. The model consists of four district subsystems: The operating profile, the rule-based energy management strategy (RB-EMS), the power plant model, and the monitoring subsystem.

6.2. Dynamic Bayesian Network Structure

Figure 5 presents the structure of the developed DBN for the pilot boat power plant case study. Root nodes represent the components of the power plant, while intermediate nodes represent noisy gates. Noisy gates are similar to logical gates of fault trees. It is assumed that the noisy gates are influenced independently by their parent nodes, resulting in a parameter reduction for the corresponding conditional probability tables and a lower computational effort [29].

Since a built-in toolbox to perform the Bayesian inference

does not exist in MATLAB libraries, the SMILE engine provided by BayesFusion was used [37]. The engine is written in C++. As a result, a wrapper was used to import the library into MATLAB.

To calculate the reliability of root nodes, the WPHM presented in the preceding sections is used. The reliability of each component is calculated using the following expression:

$$R_i(t) = e^{-\int_0^t \lambda_i(t) dt} \tag{20}$$

Root nodes are modeled as unobservable variables in the DBN. However, the components' reliability is calculated directly using equation (20). The SMILE engine supports the use of virtual evidence, where it is allowed to enter uncertain observations (i.e., reliability in this study) into normally unobservable variables [38]. Therefore, the DBN can be updated as the power plant operates at specific time intervals, feeding the root nodes with the components' reliability.

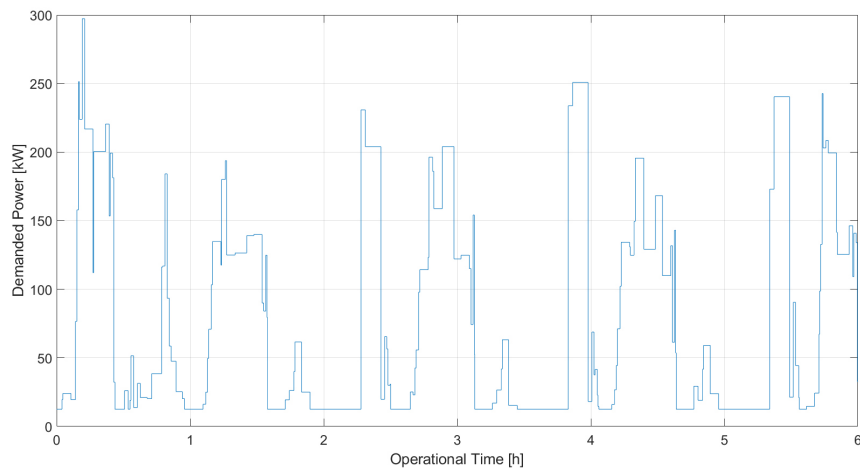


Figure 3. Sample operating profile for the propeller's power demand of the pilot boat case study

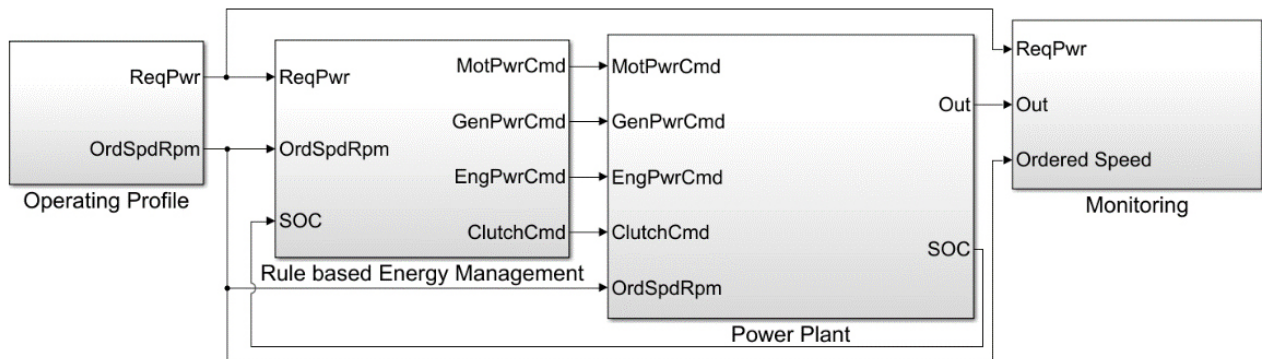


Figure 4. Screenshot of the overall model in Simulink

Finally, the shape parameters β of the Weibull distribution for each component are based on relevant experimental studies and their values are presented in Table 3.

Table 3. Weibull shape parameters

Component	β	Source
Engine	2.4	[39]
Electric machine	1.2	[40]
Battery	1.69	[41]
Gearbox	2.028	[42]

7. Results and Discussion

In this section, simulation results for the investigated hybrid power plant are presented for a one-month operational time. It must be noted that the operational time is different

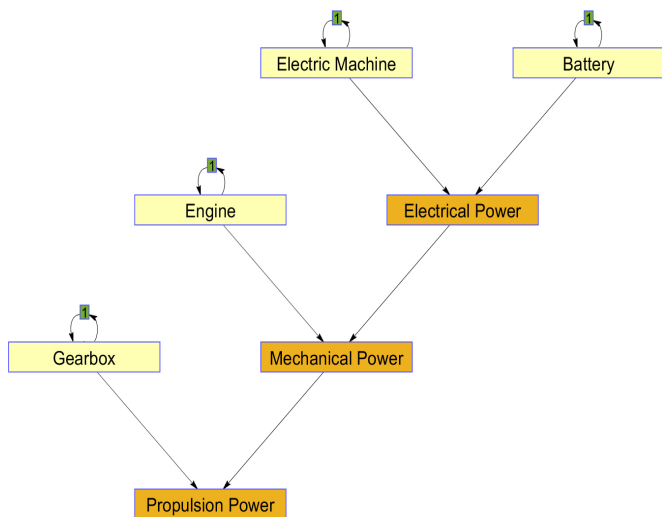


Figure 5. Developed dynamic Bayesian network structure

from the calendar time, as the former only considers the actual time the power plant operates. It was assumed that the components are initially in their healthy state. As a result, their reliability is very close to 1 (slightly less than 1 though).

Figure 6 presents the derived time variations of the components' reliability. Because of the employed time scale, fluctuations of reliability values are not noticeable in this plot; hence, a zoomed region is presented. In particular, the zoomed region presents the engine's reliability between the 28th and 29th operational days. Since the power plant is hybrid, the engine is occasionally switched off according to the rule-based energy management strategy. As a result, there are regions in the graph where the reliability remains constant.

Furthermore, an abrupt decline of the engine's reliability is observed at $t=28.3$ days, which occurs due to the engine operation in regions close to idle and full loads. Figure 7 presents the power demand and the delivered power by the engine and the electric machine in the region with the abrupt change. Results of this figure confirm that the engine operates close to the idle, which impacts the engine's reliability.

Figure 8 provides the derived time variations of the components' reliability (simulation results) as well as the time variations of the components' reliability calculated taking into account the Weibull distributions with the mean and maximum failure rate values. As observed from this figure, the derived reliability for each component is between the corresponding values calculated using the mean and the maximum failure rates. It must be noted that the engine operating time is around 13 days (instead of 30 days of operational time for other components) due to the engine switching off in several time periods.

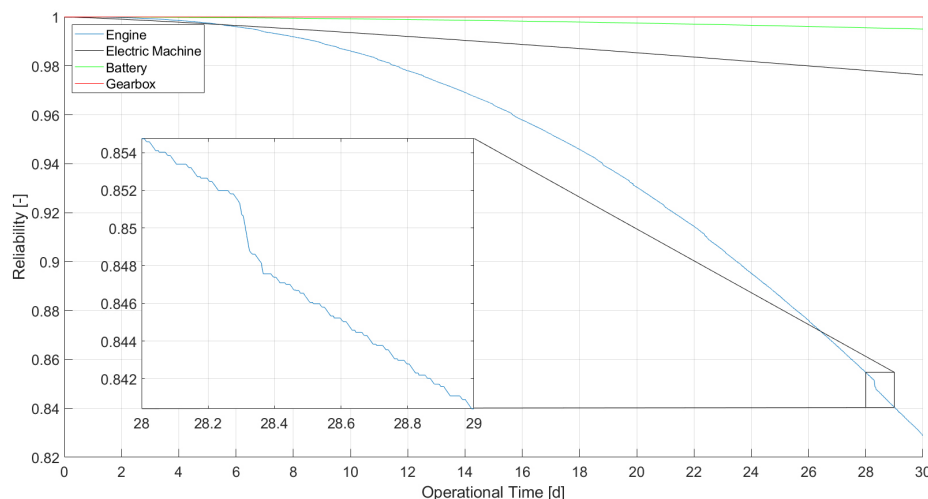


Figure 6. Derived components' reliability time variations

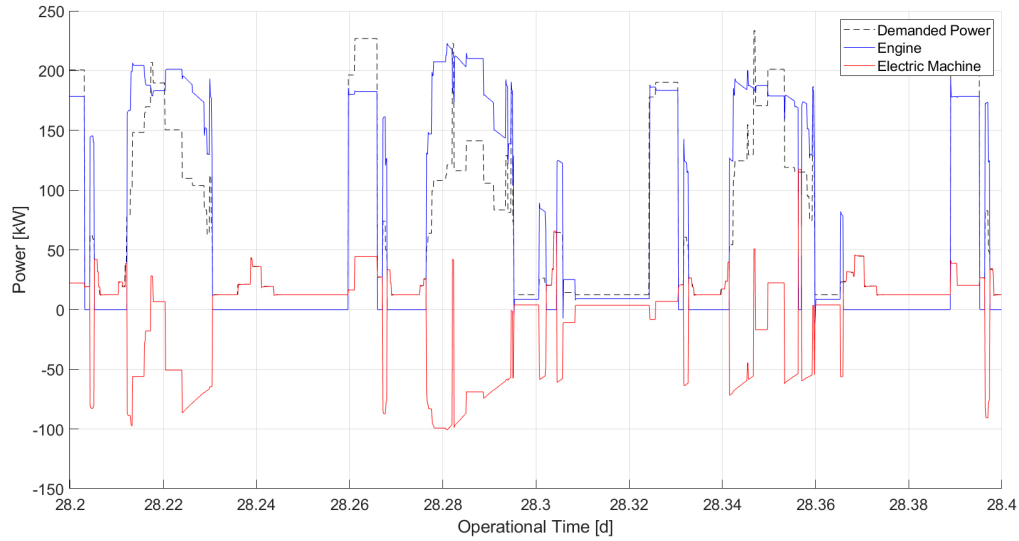


Figure 7. Power output and power demand

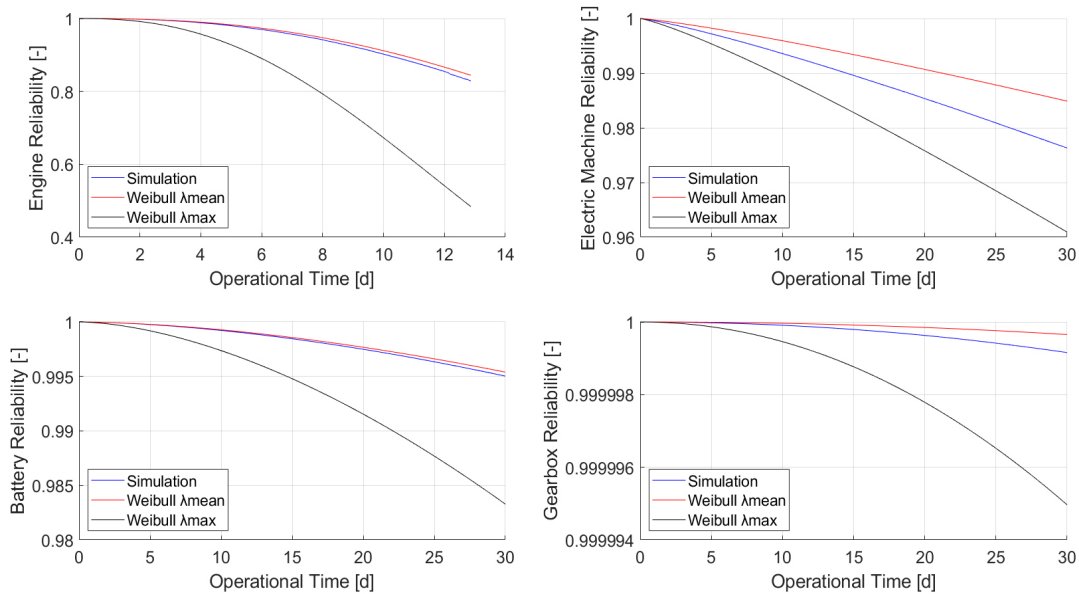


Figure 8. Comparison of the components' reliability with theoretical distributions

Finally, to demonstrate the temporal behavior of the system's reliability calculated from the developed DBN, different time slices of the dynamic Bayesian network (showing the reliability and unreliability of its components) at days 15 and 30 are presented in Figure 9. From this figure, it is inferred that the engine's unreliability exhibits the highest values (increases faster compared to other components), whereas electric components of the power plant exhibit high reliability values, thus resulting in lower values of the system's unreliability.

It must be noted that the DBN can be used as a tool to estimate the system's reliability in future time slices, considering the

current operating conditions, thus supporting the decision-making process.

8. Conclusion

In this study, a monitoring functionality for the operation of an autonomous ship power plant is proposed. The employed methodology considers operating conditions of the power plant to assess the health state of components and the system by developing and using a DBN.

Results demonstrated the usefulness of extended monitoring functionalities that include both conventional performance metrics and reliability. The latter was employed to estimate

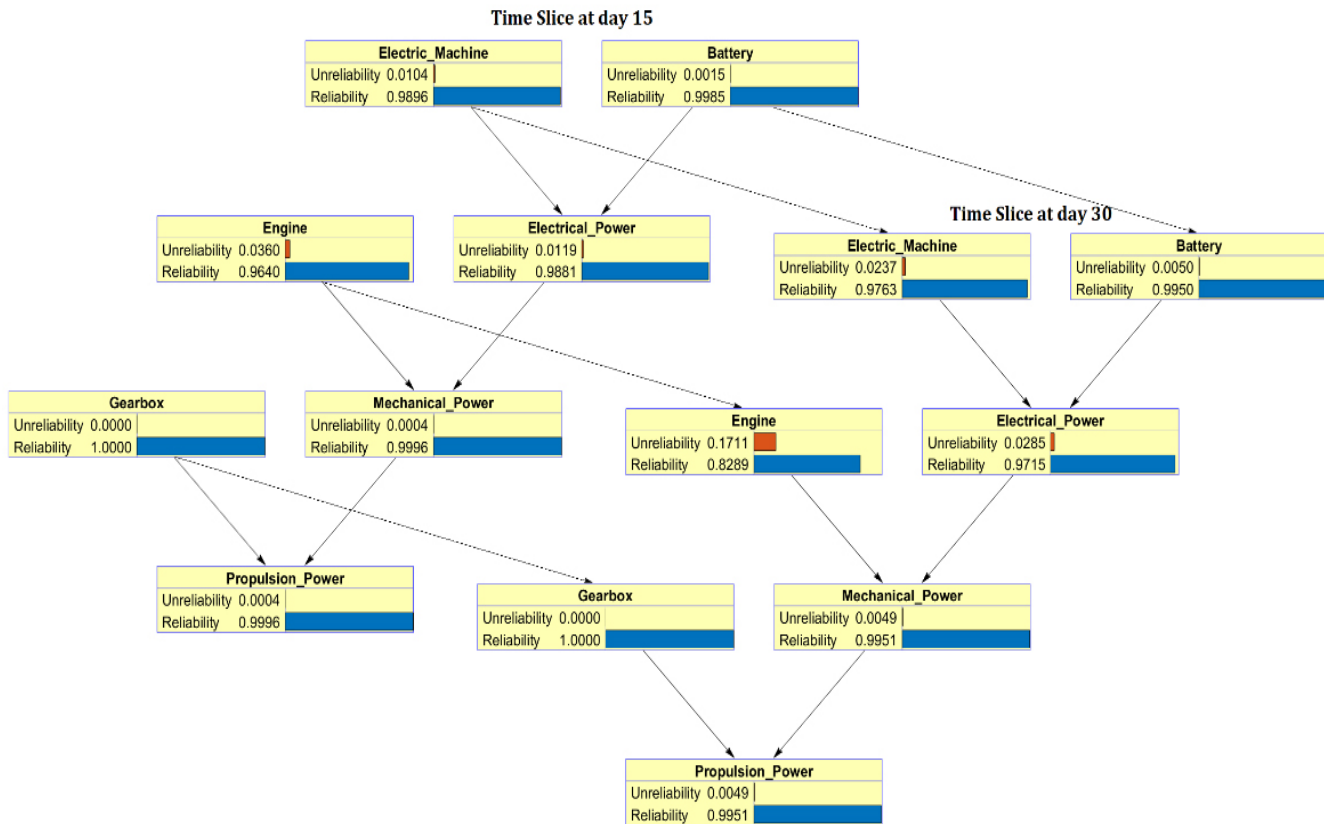


Figure 9. Time slices of the dynamic Bayesian network

the components' degradation. Future studies will include the use of this functionality as an enabling technology to develop the required automatic self-awareness of the power plant for facilitating the decision-making process in autonomous ships plants operations.

Authorship Contributions

Concept design: C. Tsoumpris, G. Theotokatos, Data Collection or Processing: C. Tsoumpris, Analysis or Interpretation C. Tsoumpris, Literature Review: C. Tsoumpris, Writing, Reviewing and Editing: C. Tsoumpris, G. Theotokatos.

Funding: The author(s) received no financial support for the research, authorship, and/or publication of this article.

References

- [1] L. Kobyliński, "Smart ships - autonomous or remote controlled?," *Zeszyty Naukowe Akademii Morskiej w Szczecinie*, vol.53, pp. 28-34, 2018.
- [2] AUTOSHIP, "D3.1 - Autonomous ship design standards," 2020. file:///C:/Users/Galenos/Desktop/AUTOSHIP_D3.1_Design-standards_v.final_13.07.2020.pdf
- [3] MUNIN, "Research in maritime autonomous systems project results and technology potentials," 2016. Available: <http://www.unmanned-ship.org/munin/wp-content/uploads/2016/02/MUNIN-final-brochure.pdf>.
- [4] S. Stoumpos, and G. Theotokatos, "A novel methodology for marine dual fuel engines sensors diagnostics and health management," *International Journal of Engine Research*, Feb 2021.
- [5] K. E. Knutsen, G. Manno, and B. J. Vartdal, "Beyond condition monitoring in the maritime industry," Jan 2014.
- [6] V. D. Nguyen et al. "A review: Prognostics and health management in automotive and aerospace," *International Journal of Prognostics and Health Management*, vol. 10, 2019.
- [7] C. Gkerekos, I. Lazakis, and G. Theotokatos, "Ship machinery condition monitoring using performance data through supervised learning," *RINA, The Royal Institution of Naval Architects, Smart Ship Technology*, Jan 2017.
- [8] I. Lazakis, Y. Raptodimos, and T. Varelas, "Predicting ship machinery system condition through analytical reliability tools and artificial neural networks," *Ocean Engineering*, vol.152, pp. 404-415, Mar 2018.
- [9] M. B. Zaman, N. Siswanto, D. Priyanta, T. Pitana, H. Prastowo, Semin, and W. Busse, "The Combination of Reliability and Predictive Tools to Determine Ship Engine Performance based on Condition Monitoring," *IOP Conf. Series: Earth and Environmental Science*, vol. 698, 2021.
- [10] G. Kökkülünk, A. Parlak, and H. H. Erdem, "Determination of performance degradation of a marine diesel engine by using curve based approach," *Applied Thermal Engineering*, vol. 108, pp. 1136-1146, Sep 2016.

- [11] W. Edge, C. Mimarest, C. Field, C. Miet, K. Walsh, and C. Miet, "The Autonomous Machinery Design of Tx Ship," *15th International Naval Engineering Conference & Exhibition*, Oct 2020. <https://doi.org/10.24868/issn.2515-818X.2020.026>
- [12] M. M. Abaei, R. Hekkenberg, and A. B. Toroody, "A multinomial process tree for reliability assessment of machinery in autonomous ships," *Reliability Engineering & System Safety*, vol. 210, pp. 107484, Jun 2021.
- [13] A. L. Ellefsen, V. Æsøy, S. Ushakov, and H. Zhang, "A comprehensive survey of prognostics and health management based on deep learning for autonomous ships," *IEEE Transactions on Reliability*, vol. 68, pp. 720-740, Apr 2019.
- [14] V. Bolbot, G. Theotokatos, R. Hamann, G. Psarros, and E. Boulougouris, "Dynamic Blackout Probability Monitoring System for Cruise Ship Power Plants," *Energies*, vol. 14, pp. 6598, Oct 2021.
- [15] I. B. Utne, A. J. Sørensen, and I. Schjøberg, "Risk management of autonomous marine systems and operations," *International Conference on Offshore Mechanics and Arctic Engineering*, vol. 3B, Sep 2017.
- [16] G. Theotokatos, "On the cycle mean value modelling of a large two-stroke marine diesel engine," *Proceedings of the Institution Mechanical Engineers, Part M: Journal of Engineering for the Maritime Environment*, vol. 224, pp. 193-205, Sep 2010.
- [17] Guzzella, and A. Sciarretta, *Vehicle propulsion systems: Introduction to modeling and optimization*, Springer, Berlin, Heidelberg, 2013.
- [18] S. Onori, L. Serrao, and G. Rizzoni, *Hybrid electric vehicles: Energy management strategies*, Springer, London, 2016.
- [19] W. L. McCarthy, W. S. Peters, and D. R. Rodger, *Marine diesel power plant practices*, Technical and Research Bulletins and Reports, pp. 3-49, 1990.
- [20] O. Tremblay, and L. A. Dessaint, "Experimental validation of a battery dynamic model for EV applications," *World Electric Vehicle Journal*, vol. 3, May 2009.
- [21] M. Jaurola, A. Hedin, S. Tikkanen, and K. Huhtala, "Optimising design and power management in energy-efficient marine vessel power systems: a literature review," *Journal of Marine Engineering & Technology*, vol. 18, pp. 92-101, 2019.
- [22] S. T. Karris, *Introduction to stateflow with applications*, Orchard Publications, 2007.
- [23] T. M. N. Bui, T. Q. Dinh, J. Marco, and C. Watts, "An energy management strategy for DC hybrid electric propulsion system of marine vessels," *2018 5th International Conference on Control, Decision and Information Technologies (CoDIT)*, pp.80-85, 2018.
- [24] K. Hein, Y. Xu, Y. Senthilkumar, W. Gary, and A. K. Gupta, "Rule-based operation task-aware energy management for ship power systems," *IET Generation Transmission & Distribution*, vol. 14, pp. 6348-6358, 2020.
- [25] M. Rausand, A. Barros, and A. Høyland, *System reliability theory: models, statistical methods, and applications*, Third Edition, 2020.
- [26] M. Zagorowska, O. Wu, J. R. Ottewill, M. Reble, and N. F. Thornhill, "A survey of models of degradation for control applications," *Annual Reviews in Control*, vol. 50, pp.150-173, 2020.
- [27] M. T. Amin, F. Khan, and S. Imtiaz, "Dynamic availability assessment of safety critical systems using a dynamic Bayesian network," *Reliability Engineering & System Safety*, vol. 178, pp. 108-117, 2018.
- [28] R. E. Neapolitan, *Learning Bayesian Networks*, Prentice hall series in artificial intelligence, Pearson, pp. 674, 2003.
- [29] A. Bobbio, L. Portinale, M. Minichino, and E. Ciancamerla, "Improving the analysis of dependable systems by mapping fault trees into Bayesian networks," *Reliability Engineering & System Safety*, vol. 71, pp. 249-260, 2001.
- [30] R. Pan, D. Lee, P. Yontay, and L. M. Sanchez, "System reliability assessment through bayesian network modeling," M. Ram, and J. P. Davim, Ed. *Advances in System Reliability Engineering*, 2019, pp. 227-241.
- [31] J. C. Salazar, P. Weber, F. Nejari, R. Sarrate, and D. Theilliol, "System reliability aware model predictive control framework," *Reliability Engineering & System Safety*, vol. 167, pp. 663-672, 2017.
- [32] D. R. Cox, "Regression Models and Life-Tables," *Journal of the Royal Statistical Society: Series B*, vol. 34, pp. 187-202, Jan 1972.
- [33] D. R. Cox, and D. Oakes, *Analysis of survival data*, Chapman and Hall/CRC, 2018, pp. 212.
- [34] N. Gorjian, L. Ma, M. Mittinty, P. Yarlagadda, and Y. Sun, "A review on reliability models with covariates," *Engineering Asset Lifecycle Management, Proceedings of the 4th World Congress on Engineering Asset Management (WCEAM 2009)*, 2009, pp.385-397.
- [35] SINTEF, and NTNU, OREDA: *Offshore and Onshore Reliability Data 6th Edition Volume 1 - Topside Equipment*, DNV GL, 2015.
- [36] W. Denson, G. Chandler, W. Crowell, and R. Wanner, *Nonelectronic Parts Reliability Data 1991*. http://www.mwfr.com/CS2/NPRD-91_a242083.pdf
- [37] BayesFusion, LLC "SMILE: Structural Modeling, Inference, and Learning Engine." [Online]. Available: <https://www.bayesfusion.com/smile/>. [Accessed: Oct. 17, 2021].
- [38] BayesFusion, LLC "GeNIe Modeler User Manual". [Online] Available: <https://support.bayesfusion.com/docs/GeNIe.pdf>. 2020.
- [39] A. K. S. Jardine, P. Ralston, N. Reid, and J. Stafford, "Proportional hazards analysis of diesel engine failure data," *Quality and Reliability Engineering International*, vol. 5, pp.207-2016, Sep 1989.
- [40] Reliability Analytics Corporation, "Failure Rate Estimates for Mechanical Components," 2019. Available: https://reliabilityanalyticstoolkit.appspot.com/mechanical_reliability_data [Accessed Oct. 21, 2021].
- [41] C. I. Ossai, and N. Raghavan, "Statistical Characterization of the State-of-Health of Lithium-Ion Batteries with Weibull Distribution Function-A Consideration of Random Effect Model in Charge Capacity Decay Estimation," *Batteries*, vol. 3, pp. 32, Oct. 2017.
- [42] S. Dutta, D. Kumar, and P. Kumar, "Reliability analysis of defence vehicles gear box assembly under preventive maintenance," *Indian Journal of Science and Technology*, vol. 3, pp. 328-331, 2010.